

1 Greenhouse gas fluxes in mangrove forest soil in an Amazon estuary

2 Saúl Edgardo Martínez Castellón¹, José Henrique Cattanio^{1*}, José Francisco Berrêdo^{1,3},
3 Marcelo Rollnic², Maria de Lourdes Ruivo^{1,3}, Carlos Noriega².

4 ¹ Graduate Program in Environmental Sciences. Federal University of Pará, Belém,
5 Brazil

6 ² Marine Environmental Monitoring Research Laboratory. Federal University of Pará,
7 Belém, Brazil.

8 ³ Department of Earth Sciences and Ecology. Paraense Emílio Goeldi Museum, Belém,
9 Brazil

10 * Corresponding author: cattanio@ufpa.br (J.H. Cattanio)

11 Abstract: Tropical mangrove forests are important carbon sinks, the soil being the main
12 carbon reservoir. Understanding the variability and the key factors that control fluxes is
13 critical to accounting for greenhouse gas (GHG) emissions, particularly in the current
14 scenario of global climate change. This study is the first to quantify carbon dioxide
15 (CO₂) and methane (CH₄) ~~and carbon dioxide (CO₂)~~ emissions using a dynamic
16 chamber in a natural mangrove soil of the Amazon. The plots for the trace gases study
17 were allocated at contrasting topographic heights. The results showed that the mangrove
18 soil of the Amazon estuary is a source of CO₂ (6.66 g CO₂ m⁻² d⁻¹) and CH₄ (0.13 g CH₄
19 m⁻² d⁻¹) to the atmosphere. The CO₂ flux was higher in the high topography (7.~~858-86~~ g
20 CO₂ m⁻² d⁻¹) than in the low topography (4.734 g CO₂ m⁻² d⁻¹) in the rainy season, and
21 CH₄ was higher in the low topography (0.~~128-13~~ g CH₄ m⁻² d⁻¹) than in the high
22 topography (0.014 g CH₄ m⁻² d⁻¹) in the dry season. However, in the dry period, the low
23 topography soil produced more CH₄. Soil organic matter, carbon and nitrogen ratio
24 (C/N), and redox potential influenced the annual and seasonal variation of CO₂
25 emissions; however, they did not affect CH₄ fluxes. The mangrove soil of the Amazon
26 estuary produced 35.40 Mg CO_{2-eq} ha⁻¹ y⁻¹. A total of 2.16 kg CO₂ m⁻² y⁻¹ needs to be
27 sequestered by the mangrove ecosystem to counterbalance CH₄ emissions.

28 1 Introduction

29 ~~M~~The mangrove areas are estimated to be the main contributors to greenhouse gas
30 emissions in marine ecosystems (Allen et al., 2011; Chen et al., 2012). However,
31 mangrove forests are highly productive due to a high nutrient turnover rate (Robertson
32 et al., 1992) and have mechanisms that maximize carbon gain and minimize water loss
33 through plant transpiration (Alongi and Mukhopadhyay, 2015). A study conducted in 25
34 mangrove forests (between 30° latitude and 73° longitude) revealed that these forests

35 | are the richest in carbon (C) storage in the tropics, containing on average 1,023 Mg C
36 | ha⁻¹ of which 49 to 98% is present in the soil (Donato et al., 2011).

37 | The estimated soil CO₂ outgassing flux, in tropical estuarine areas is 16.2 Tg C y⁻¹
38 | (Alongi, 2009). However, soil efflux measurements from tropical mangroves revealed
39 | emissions ranging from 2.9 to 11.0 g CO₂ m⁻² d⁻¹ (Castillo et al., 2017; Chen et al.,
40 | 2014; Shiau and Chiu, 2020). In situ CO₂ production is related to the water input of
41 | terrestrial, riparian, and groundwater brought by rainfall (Rosentreter et al., 2018b). Due
42 | to the periodic tidal movement, the mangrove ecosystem is daily flooded, leaving the
43 | soil anoxic and consequently reduced, favoring methanogenesis (Dutta et al., 2013).
44 | Thus, estuaries are considered hotspots for CH₄ production and emission (Bastviken et
45 | al., 2011; Borges et al., 2015). ~~The~~ organic material decomposition by methanogenic
46 | bacteria in anoxic environments, such as sediments, inner suspended particles,
47 | zooplankton gut (Reeburgh, 2007; Valentine, 2011), and the impact of freshwater
48 | should change the electron flow from sulfate-reducing bacteria to methanogenesis
49 | (Purvaja et al., 2004), which also results in CH₄ formation. On the other hand, ~~an~~
50 | ~~ecosystem with high~~ salinity levels, above 18 ppt, may ~~show result in~~ an absence of CH₄
51 | emissions (Poffenbarger et al., 2011), since ~~methane~~ CH₄ dissolved in pores is typically
52 | oxidized anaerobically by sulfate (Chuang et al., 2016). Currently the uncertainty in
53 | emitted CH₄ values in vegetated coastal wetlands is approximately 30% (EPA, 2017).
54 | Soil flux measurements from tropical mangroves revealed emissions rangeing from 0.3
55 | to 4.4 mg CH₄ m⁻² d⁻¹ (Castillo et al., 2017; Chen et al., 2014; Kreuzwieser et al., 2003).

56 | The production of greenhouse gases from soils is mainly driven by biogeochemical
57 | processes. Microbial activities and gas production are related to soil properties,
58 | including total carbon and nitrogen concentrations, moisture, porosity, salinity, and
59 | redox potential (Bouillon et al., 2008; Chen et al., 2012). Due to the dynamics of tidal
60 | movements, mangrove soils may become saturated and present ~~a~~ reduced oxygen
61 | availability, or suffer total aeration caused by the ebb tide. Studies attribute soil carbon
62 | flux responses to moisture perturbations because of seasonality and flooding events
63 | (Banerjee et al., 2016), with fluxes being dependent on tidal extremes (high tide and low
64 | tide), and flood duration (Chowdhury et al., 2018). In addition, phenolic compounds
65 | inhibit microbial activity and help keep organic carbon intact, thus leading to the
66 | accumulation of organic matter in mangrove forest soils (Friesen et al., 2018).

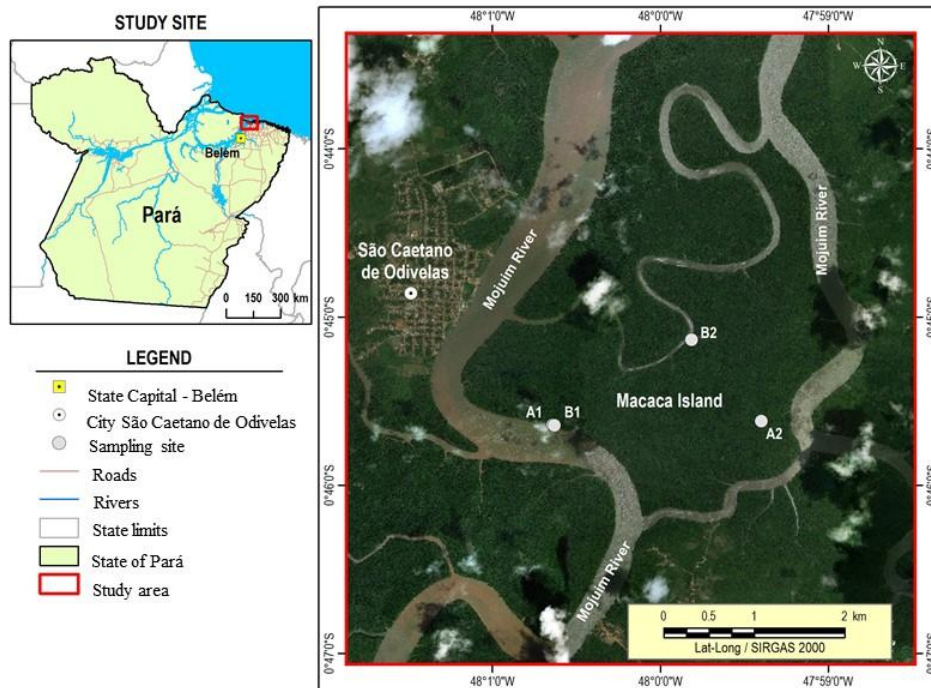
Formatado: Subscrito

67 The Amazonian coastal areas in the State of Pará (Brazil) cover 2,176.8 km² where
68 mangroves develop under the macro-tide regime (Souza Filho, 2005), representing
69 approximately 85% of the entire area of Brazilian mangroves (Herz, 1991). The
70 objective of this study is to investigate the monthly flux of CO₂ and CH₄ from the soil,
71 at two topographic heights, in a pristine mangrove area in the Mojuim River Estuary,
72 belonging to the Amazon biome. The gas fluxes were studied together with the analysis
73 of the vegetation structure and soil physical-chemical parameters.

74 2 Material and Methods

75 2.1 Study site

76 This study was conducted in the Amazonian coastal zone, Macaca Island (-0.746491
77 latitude and -47.997219 longitude), located in the Mojuim River estuary, at the
78 Mocapajuba Marine Extractive Reserve, municipality of São Caetano de Odivelas
79 (Figure 1), state of Pará (Brazil). The Macaca island has an area of 1,322 ha of pristine
80 mangroves, ~~which-and~~ belongs to a mangrove area of 2,177 km² in the state of Pará
81 (Souza Filho, 2005). The climate is type Am (tropical monsoon) according to the
82 Köppen classification (Peel et al., 2007). The climatological data were obtained from
83 the Meteorological Database for Teaching and Research of the National Institute of
84 Meteorology (INMET). The area has a rainy season from January to June (2,296 mm of
85 precipitation) and a dry season from July to December (687 mm). March and April were
86 the rainiest months with 505 and 453 mm of precipitation, while October and November
87 were the driest (53 and 61 mm, respectively). The minimum temperatures occur in the
88 rainy period (26 °C) and the maximum in the dry period (29 °C). The Mojuim estuary
89 has a macrotidal regime, with an average amplitude of 4.9 m during spring tide and 3.2
90 m during low tide (Rollnic et al., 2018). During the wet season the Mojuim River has a
91 flow velocity of 1.8 m s⁻¹ at the ebb tide and 1.3 m s⁻¹ at the flood tide, ~~whereas in-~~
92 ~~During~~ the dry season, the maximum currents reach 1.9 m s⁻¹ at the flood and 1.67 m s⁻¹
93 at the ebb tide (Rocha, 2015). The annual mean salinity is 26.95 PSU (Valentim et al.,
94 2018).



95

96 Figure 1. The Macaca Island located in the mangrove coast of Northern Brazil,
 97 Municipality of São Caetano de Odivelas (state of Pará), with sampling points at low
 98 (plot B1 and plot B2) and high (plot A1 and plot A2) topographies ~~(plot A1 and plot~~
 99 ~~A2)~~. Image Source: © Google Earth

100 The Mojuim River region is geomorphologically formed by partially submerged river
 101 basins consequent of the increase in the relative sea level during the Holocene (Prost et
 102 al., 2001) associated with the formation of mangroves, dunes, and beaches (El-Robrini
 103 et al., 2006). ~~This river forms the entire watershed of the municipality of São Caetano~~
 104 ~~de Odivelas and borders the municipality of São João da Ponta (Figure 1).~~ Before
 105 reaching the estuary, the Mojuim River crosses an area of a dryland forest highly
 106 fragmented by family farming, forming remnants of secondary forest (< 5.0 ha) of
 107 various ages (Fernandes and Pimentel, 2019). The population economically exploited
 108 the estuary, primarily by artisanal fishing, crab (*Ucides cordatus* L.) extraction, and
 109 oyster farms.

110 The flora of the mangrove area of Macaca Island is little anthropized and comprises the
 111 plant genera *Rhizophora*, *Avicenia*, *Laguncularia*, and *Acrostichum* (Ferreira, 2017;
 112 França et al., 2016). The estuarine plains are influenced by macrotide dynamics and can

[C1] Comentário: I think this information is unnecessary, as you cannot see São João da Ponta in Figure 1.

113 | be physiographically divided into four sectors according to the different vegetation
114 | covers, associated with the landforms distribution, topographic gradient, tidal
115 | inundation, and levels of anthropic transformation-(França et al., 2016). The Macaca
116 | Island is ranked as being from the fourth sector, which implies having woods of adult
117 | trees of the genus *Ryzophora* with an average height of 10 to 25 m, being-is located at
118 | an elevation of 0 to 5 m, and having silt-clay soil (França et al., 2016).

119 | Four sampling plots were selected in the Macaca Island (Figure 1) on 19/05/2017, when
120 | the moon was in the waning quarter phase: two plots where flooding occurs every day
121 | (plots B1 and B2; Figure 1), called low topography (Top_Low), and two plots where
122 | flooding occurs only at high tides during the solstice and on the high tides of the rainy
123 | season of the new and full moons (plots A1 and A2; Figure 1), called high topography
124 | (Top_High).

125 | 2.2 Greenhouse gas flux measurements

126 | In each plot, eight Polyvinyl Chloride rings with 0.20 m diameter and 0.12 m height
127 | were randomly installed within a circumference with a diameter of 20 m. The rings had
128 | an area of 0.028 m² (volume of 3.47 L), were fixed 0.05 m into the ground, and
129 | remained in place until the study was completed. Once a month, gas fluxes were the
130 | Greenhouse gas flux was measured during periods of waning or crescent moon, as these
131 | are the times when the soil in the low topography is more exposed. To avoid the
132 | influence of mangrove roots on the gas fluxes, the rings were placed in locations
133 | without any seedlings or aboveground mangrove roots. The CO₂ and CH₄
134 | concentrations (ppm) were measured using the dynamic chamber methodology
135 | (Norman et al., 1997; Verchot et al., 2000), sequentially connected to a Los Gatos
136 | Research portable gas analyzer (Mahesh et al., 2015). The device was calibrated
137 | monthly with a high quality standard gas (500 ppm CO₂; 5 ppm CH₄). The rings were
138 | sequentially closed for three minutes with a PVC cap, being connected to the analyzer
139 | through two 12.0 m polyethylene hoses. The gas concentration was measured every two
140 | seconds and automatically stored by the analyzer. CO₂ and CH₄ fluxes were calculated
141 | from the linear regression of increasing/decreasing CO₂ and CH₄ concentrations within
142 | the chamber, usually between one and three minutes after the ring cover was placed
143 | (Frankignoulle, 1988; McEwing et al., 2015). The flux is considered zero when the
144 | linear regression reaches an R² < 0.30 (Sundqvist et al., 2014). However, in our
145 | analyses, most regressions reached R² > 0.70, and the regressions were weak and

146 considered zero in only 6% of the samples. At the end of each flux measurement, the
147 height of the ring above ground was measured at four equidistant points with a ruler.
148 The seasonal data were analyzed by comparing the average monthly fluxes in the wet
149 season and dry season separately.

150 **2.3 Vegetation structure and biomass**

151 The floristic survey was conducted in October 2017 using circular 1,256.6 m² plots
152 (Kauffman et al., 2013) divided into four 314.15 m² subplots, which is the equivalent to
153 0.38 ha (~~Figure 1~~), at the same topographies as the gas flux analysis ([Figure 1](#)). We
154 recorded the diameter above the aerial roots, the diameter of the stem, and total height
155 of all trees with DBH (diameter at breast height; m) greater than 0.05m. The allometric
156 equations (Howard et al., 2014) to calculate tree biomass (aboveground biomass; AGB)
157 were: $AGB = 0.1282 * DBH^{2.6}$ ($R^2 = 0.92$) for *R. mangle*; $AGB = 0.140 * DBH^{2.4}$ ($R^2 =$
158 0.97) for *A. germinans*; and $Total\ AGB = 0.168 * \rho * DBH^{2.47}$ ($R^2 = 0.99$), where ρ_R
159 $mangle = 0.87$; $\rho_{A. germinans} = 0.72$ ($\rho =$ wood density).

160 **2.4 Soil sampling and environmental characterization**

161 Four soil samples were collected with an auger at a depth of 0.10 m in all the studied
162 plots for gas flux measurements ([Figure 1](#)) in July 2017 (beginning of the dry season)
163 and January 2018 (beginning of the rainy season; ~~Figure 1~~). Before the soil samples
164 were removed, pH and redox potential (Eh; mV) were measured with a Metrohm 744
165 equipment by inserting the platinum probe directly into the intact soil at a depth of 0.10
166 m (Bauza et al., 2002). The soil samples collected in the field were transported to the
167 laboratory (Chemical Analysis Laboratory of the *Museu Paraense Emílio Goeldi*) in
168 thermal boxes containing ice. The soil samples were analyzed on the day after collection
169 at the laboratory, and the samples were kept in a freezer. Salinity (Sal; ppt) was
170 measured with PCE-0100, and soil moisture (Sm; %) by the residual gravimetric
171 method (EMBRAPA, 1997).

172 Organic Matter (OM; g kg⁻¹), Total Carbon (TC; g kg⁻¹) and Total Nitrogen (TN; g kg⁻¹)
173 were calculated by volumetry (oxidoreduction) using the Walkley-Black method
174 (Kalembasa and Jenkinson, 1973). Microbial carbon (C_{mic}; mg kg⁻¹) and microbial
175 nitrogen (N_{mic}; mg kg⁻¹) were determined through the 2.0 min of Irradiation-extraction
176 method of soil by microwave technique (Islam and Weil, 1998). Microwave heated soil
177 extraction proved to be a simple, fast, accurate, reliable, and safe method to measure

178 soil microbial biomass (Araujo, 2010; Ferreira et al., 1999; Monz et al., 1991). The C_{mic}
179 was determined by dichromate oxidation (Kalembasa and Jenkinson, 1973; Vance et al.,
180 1987). The N_{mic} was analyzed following the method described by Brookes et al. (1985),
181 changing fumigation to irradiation, which uses the difference between the amount of T_N
182 in irradiated and non-irradiated soil. We used the flux conversion factor of 0.33
183 (Sparling and West, 1988) and 0.54 (Almeida et al., 2019; Brookes et al., 1985), for
184 carbon and nitrogen, respectively. Particle size analysis was performed separately on
185 four soil samples collected at each flux plot, in the two seasons (October 2017 and
186 March 2018), according to EMBRAPA (1997).

187 At each gas flux measurement, environmental variables such as air temperature (T_{air} ,
188 °C), relative humidity (RH, %), and wind speed (W_s , $m\ s^{-1}$) were quantified with a
189 portable thermo-hygrometer (model AK821) at the height of 2.0 m above the soil
190 surface. Soil temperature (T_s , °C) was measured with a portable digital thermometer
191 (model TP101) after each gas flux measurement. Daily precipitation was obtained from
192 an automatic precipitation station installed at a pier on the banks of the Mojuim River in
193 São Caetano das Odivelas (coordinates: -0.738333 latitude; -48.013056 longitude).

194 **2.5 Statistical analyses**

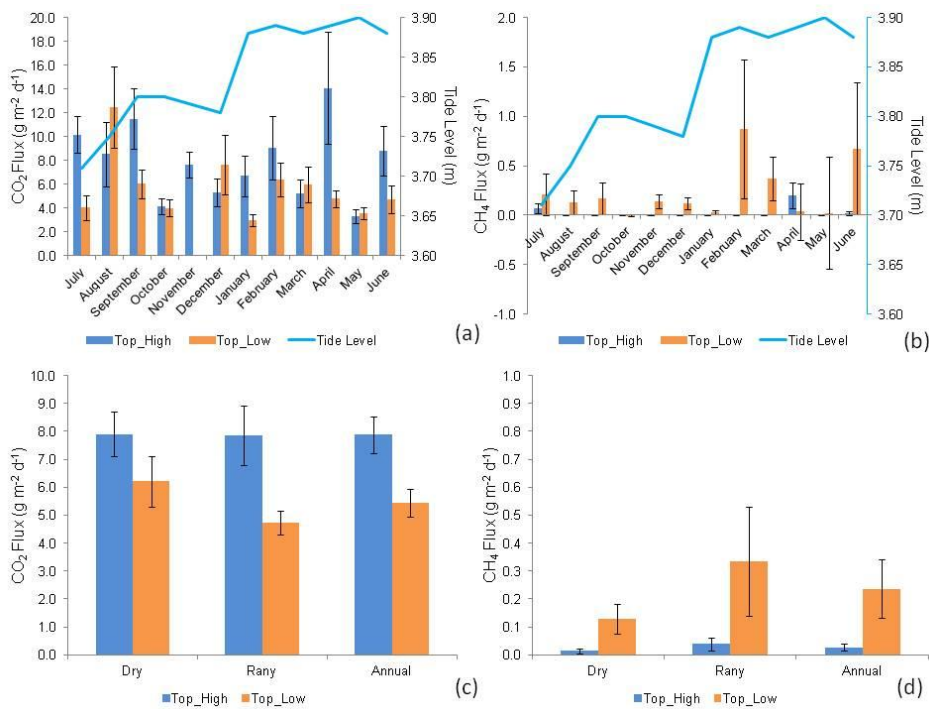
195 On the Macaca Island, two treatments were allocated (low and high topography), with
196 two plots in either treatment. In each plot, eight chambers were randomly distributed,
197 which were considered sample repetitions. The normality of the data of FCH_4 and F
198 FCO_2 flux, and soil physicochemical parameters was evaluated using the Shapiro-Wilks
199 method. The soil CO_2 and CH_4 flux showed a non-normal distribution. Therefore, we
200 used the non-parametric ANOVA (Kruskal-Wallis, $p < 0.05$) to test the differences
201 between the two treatments among months and seasons. The physicochemical
202 parameters were normally distributed. Therefore, a parametric ANOVA was used to test
203 the statistical differences ($p < 0.05$) between the two treatments among months and
204 seasons. Pearson correlation coefficients were calculated to determine the relationships
205 between soil properties and gas fluxes in the months (dry and wet season) when the
206 chemical properties of the soil were analyzed at the same time as gas fluxes were
207 measured. Statistical analyses were performed with the free statistical software Infostat
208 2015®.

209 **3 Results**

210 **3.1 Carbon dioxide and methane fluxes**

211 CO₂ fluxes differed significantly between topographies only in January (H = 3.915; p =
 212 0.048), July (H = 9.091; p = 0.003), and November (H = 11.294; p < 0.00001) (Figure
 213 2; Supplementary Information, SI 1), with generally higher fluxes at the high
 214 topography than at the low topography. At the high topography, CO₂ fluxes were
 215 significantly higher (H = 24.510; p = 0.011) in July compared to August and December,
 216 March, October, and May, not differing from the other months of the year. Similarly, at
 217 the low topography, CO₂ fluxes were statistically higher (H = 19.912; p = 0.046) in
 218 September and February than in January and November, not differing from the other
 219 months. We found a mean monthly flux of 327.9 ± 780.0 mg CO₂ m⁻² hd⁻¹ (mean ±
 220 standard error) and 2175.2 ± 510.0 mg CO₂ m⁻² hd⁻¹ at the high and low
 221 topographies, respectively.

222



223

224 Figure 2. CO₂ (a) and CH₄ (b) fluxes (g CO₂ or CH₄ m⁻² d⁻¹) monthly (July 2018 to June
 225 2019) (n = 16). Seasonal (Dry and Rainy) and annual fluxes of CO₂ (c) and CH₄ (d), at

226 high (Top_High) and low (Top_Low) topographies (n = 96), in a mangrove forest soil
227 compared to tide level (Tide Level). The bars represent the standard error of the mean.

228 The CH₄ fluxes were statistically different between topographies only in November (H
229 = 9.276; p = 0.002) and December (H = 4.945; p = 0.005), with higher fluxes at the low
230 topography (Figure 2; SI 1). At the high topography, CH₄ fluxes were significantly (H =
231 40.073; p < 0.001) higher in April and July compared to the other months studied, and
232 in November CH₄ was consumed from the atmosphere (Figure 2; SI 1). Similarly, CH₄
233 fluxes at the low topography did not vary significantly among months (H = 10.114; p =
234 0.407).

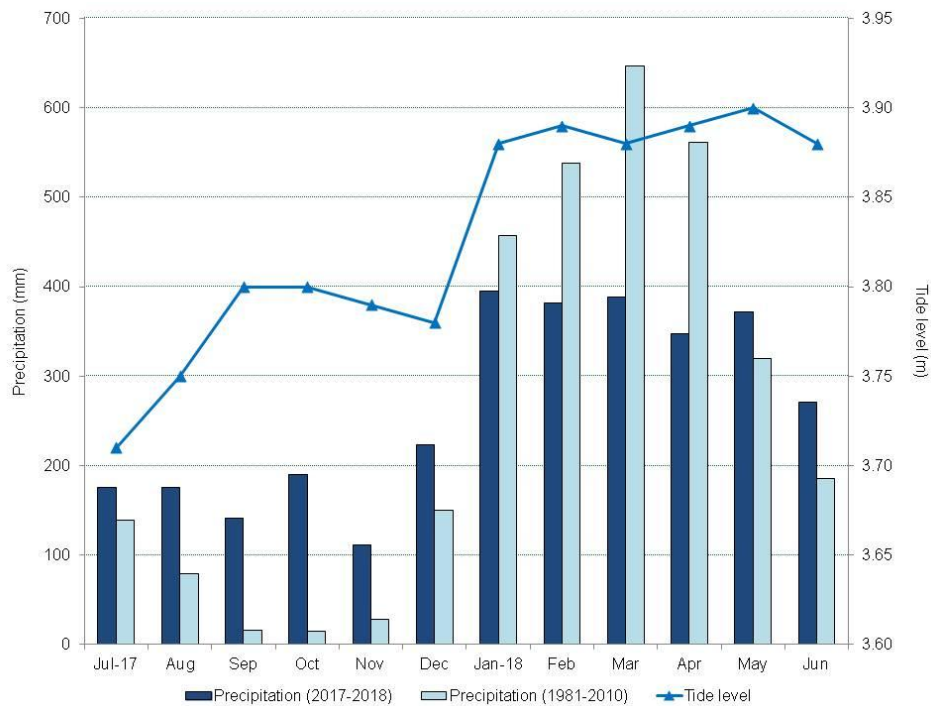
235 Greenhouse gas fluxes (Figure 2) were only significantly different between
236 topographies in the dry season (Figure 3), period when CO₂ fluxes were higher (H =
237 7.378; p = 0.006) at the high topography and CH₄ fluxes at the low topography (H =
238 8.229; p < 0.001). In the Macaca Island, the mean annual fluxes of CO₂ and CH₄ were
239 6.659 ± 0.419 g CO₂ m⁻² d⁻¹ and 0.132 ± 0.053 g CH₄ m⁻² d⁻¹, respectively. During the
240 study year, the CO₂ flux from the mangrove soil ranged from -5.06 to 68.96 g CO₂ m⁻²
241 d⁻¹ (mean 6.66 g CO₂ m⁻² d⁻¹), while the CH₄ flux ranged from -5.07 to 11.08 g CH₄ m⁻²
242 d⁻¹ (mean 0.13 g CH₄ m⁻² d⁻¹), resulting in a total carbon rate of 1.92 g C m⁻² d⁻¹ or 7.00
243 Mg C ha⁻¹ y⁻¹ (Figure 2).

244 3.2 Weather data

245 There was a marked seasonality during the study period (Figure 2), with 2,155.0 mm of
246 precipitation during the rainy period and 1,016.5 mm during the dry period. The highest
247 tides occurred in the period of greater precipitation (Figure 3) due to the rains. However,
248 the rainfall distribution was different from the climatological normal (Figure 3). The
249 precipitation in the rainy season was 553.2 mm below and in the dry season was 589.1
250 mm above the climatological normal. Thus, in the period studied, the dry season was
251 rainier and the rainy season drier than the climatological normal, which may be a
252 consequence of ~~global climate change~~ the La Niña event (Wang et al., 2019).

253

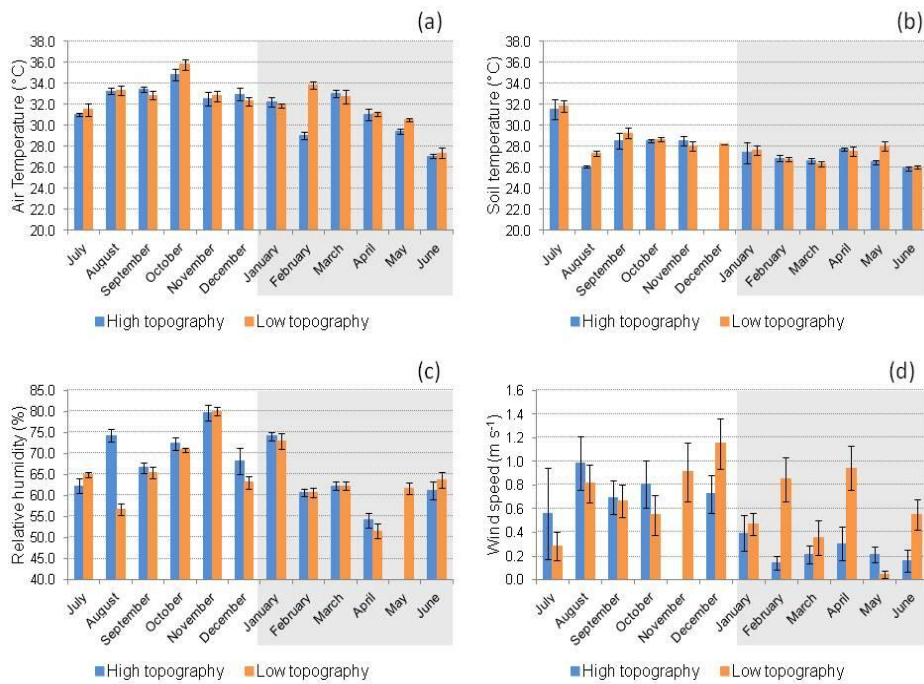
Formatado: Fonte: Itálico



254

255 Figure 3. Monthly climatological normal in the municipality of Soure (1981-2010, mm),
 256 monthly precipitation (mm), and maximum tide height (m) from 2017 to 2018, in the
 257 municipality of São Caetano de Odivelas (PA).

258 T_{air} was significantly higher (LSD = 0.72, $p = 0.01$) at the high (31.24 ± 0.26 °C) than at
 259 the low topography (30.30 ± 0.25 °C) only in the rainy season (Figure 4a). No
 260 significant variation in T_s was found between topographies in either season (Figure 4b).
 261 RH was significantly higher (LSD = 2.55, $p = 0.01$) at the high topography ($70.54 \pm$
 262 0.97%) than at the low topography ($66.85 \pm 0.87\%$) only in the rainy season (Figure 4c).
 263 W_s (Figure 4d) was significantly higher (LSD = 0.15, $p < 0.00$) at the low (0.54 ± 0.06
 264 $m s^{-1}$) than at the high topography ($0.24 \pm 0.04 m s^{-1}$) also in the rainy season.



265

266 Figure 4. a) Air temperature (°C), b) soil temperature (°C), c) relative humidity (%), and
 267 d) wind speed (m s⁻¹) at high and low topographies, from July 2017 to June 2018 in a
 268 mangrove area in the Mojuim River estuary. Bars highlighted in grey correspond to the
 269 rainy season (n = 16). The bars represent the standard error.

270 3.3 Soil characteristics

271 Silt concentration was higher at the low topography (LSD: 14.763; p= 0.007) and clay
 272 concentration was higher at the high topography plots (LSD: 12.463; p= 0.005), in both
 273 seasons studied (Table 1). Soil particle size analysis did not differ statistically (p > 0.05)
 274 between the two seasons (Table 1). Soil moisture did not vary significantly (p > 0.05)
 275 between topographies at each season, or between seasonal periods at the same
 276 topography (Table 1). The pH varied statistically (LSD: 5.950; p= 0.006) only at the
 277 low topography when the two seasons were compared, being more acidic in the dry
 278 period (Table 1). The pH values were significantly (LSD: 0.559; p= 0.008) higher in the
 279 dry season (Table 1). No variation in Eh was identified between topographies and
 280 seasons (Table 1), although it was higher in the dry season than in the rainy season.
 281 However, Sal values were higher (LSD: 3.444; p = 0.010) at the high topography than at

282 the low topography in the dry season (Table 1). In addition, Sal was significantly higher
283 in the dry season than in the rainy season, in both high (LSD: 2.916; $p < 0.001$) and low
284 (LSD: 3.003; $p < 0.001$) topographies (Table 1). (Table 1).

285 Table 1. Analysis of Sand (%), Silt (%), Clay (%), Moisture (%), pH, Redox Potential (Eh, mV) and salinity (Sal; ppt) in the mangrove soil of
 286 high and low topographies, and in the rainy and dry seasons (Macaca island, São Caetano das Odivelas). Numbers represent the mean \pm standard
 287 error of the mean. Lower case letters compare topographies in each seasonal period and upper-case letters compare the same topography between
 288 seasonal periods. Different letters indicate statistical difference (LSD, $p < 0.05$).

Season	Topography	Sand (%)	Silt (%)	Clay (%)	Moisture (%)	pH	Eh (mV)	Sal (ppt)
Dry	High	12.1 \pm 1.4 ^{aA}	41.8 \pm 3.3 ^{bA}	46.1 \pm 2.6 ^{aA}	73.1 \pm 6.6 ^{aA}	5.5 \pm 0.2 ^{aA}	190.25 \pm 45.53 ^{aA}	35.25 \pm 1.11 ^{aA}
	Low	9.7 \pm 2.5 ^{aA}	63.6 \pm 6.1 ^{aA}	26.6 \pm 5.2 ^{bA}	86.9 \pm 3.4 ^{aA}	5.3 \pm 0.3 ^{aA}	106.38 \pm 53.76 ^{aA}	30.13 \pm 1.16 ^{bA}
	Mean	10.9 \pm 1.4 ^A	52.7 \pm 4.4 ^A	36.4 \pm 3.8 ^A	80.0 \pm 4.0 ^A	5.4 \pm 0.2 ^A	148.31 \pm 35.71 ^A	32.69 \pm 1.02 ^A
Rainy	High	12.1 \pm 1.4 ^{aA}	41.8 \pm 3.3 ^{bA}	46.1 \pm 2.6 ^{aA}	88.9 \pm 3.5 ^{aA}	4.9 \pm 0.4 ^{aA}	92.50 \pm 56.20 ^{aA}	7.50 \pm 0.78 ^{aB}
	Low	9.7 \pm 2.5 ^{aA}	63.6 \pm 6.1 ^{aA}	26.6 \pm 5.2 ^{bA}	88.6 \pm 3.7 ^{aA}	4.4 \pm 0.1 ^{aB}	36.25 \pm 49.97 ^{aA}	8.13 \pm 0.79 ^{aB}
	Mean	10.9 \pm 1.4 ^A	52.7 \pm 4.4 ^A	36.4 \pm 3.8 ^A	88.7 \pm 2.5 ^A	4.6 \pm 0.2 ^B	64.38 \pm 37.04 ^A	7.81 \pm 0.54 ^B

289

290 The C_{mic} did not differ between topographies in the two seasons (Table 2). However, T_C
291 was significantly higher in the low topography in the dry season (LSD: 5.589; $p <$
292 0.000) and in the rainy season (LSD: 5.777; $p = 0.024$). In addition, C_{mic} was higher in
293 the dry season in both the high (LSD: 11.325; $p < 0.010$) and low (LSD: 9.345; $p <$
294 0.000) topographies (Table 2). N_{mic} did not vary between topographies seasonally.
295 However, N_{mic} in the high (LSD: 9.059; $p = 0.013$) and low topographies (LSD: 4.447;
296 $p = 0.001$) was higher during the dry season (Table 2). The C/N ratio (Table 2) was
297 higher in the low than in the high topography in both the dry (LSD: 3.142; $p < 0.000$)
298 and rainy seasons (LSD: 3.675; $p = 0.033$). However, only in the low topography was
299 the C/N ratio higher (LSD: 1.863; $p < 0.000$) in the dry season than in the rainy season
300 (Table 2). Soil OM was higher at the low topography in the rainy (LSD: 9.950; $p <$
301 0.024) and in the dry seasons (LSD: 9.630; $p < 0.000$). However, only in the lowland
302 topography was the OM concentration higher in the dry season than in the rainy season
303 (Table 2).

304 Table 2. Seasonal and topographic variation in microbial Carbon (C_{mic} ; $mg\ kg^{-1}$), microbial Nitrogen (N_{mic} , $mg\ kg^{-1}$), Total Carbon (T_C ; $g\ kg^{-1}$),
 305 Total Nitrogen (N_T ; $g\ kg^{-1}$), Carbon/Nitrogen ratio (C/N) and Soil Organic Matter (OM; $g\ kg^{-1}$). Numbers represent the mean (\pm standard error).
 306 Lower case letters compare topographies at each season, and upper-case letters compare the topography between seasons.

Season	Topography	C_{mic} $mg\ kg^{-1}$	N_{mic} $mg\ kg^{-1}$	T_C $g\ kg^{-1}$	T_N $g\ kg^{-1}$	C/N	OM $g\ kg^{-1}$
Dry	High	22.12 \pm 5.22 ^{aA}	12.76 \pm 4.20 ^{aA}	14.12 \pm 2.23 ^{bA}	1.43 \pm 0.06 ^{aA}	9.60 \pm 1.20 ^{bA}	24.35 \pm 3.84 ^{bA}
	Low	26.34 \pm 4.23 ^{aA}	10.34 \pm 2.05 ^{aA}	26.44 \pm 1.35 ^{aA}	1.56 \pm 0.04 ^{aA}	16.98 \pm 0.84 ^{aA}	45.59 \pm 2.32 ^{aA}
	Mean	24.23 \pm 3.29 ^A	11.55 \pm 2.28 ^A	20.28 \pm 2.03 ^A	1.49 \pm 0.04 ^A	13.29 \pm 1.19 ^A	34.97 \pm 3.50 ^A
Rainy	High	7.40 \pm 0.79 ^{aB}	0.75 \pm 0.41 ^{aB}	11.46 \pm 2.48 ^{bA}	1.32 \pm 0.04 ^{aA}	8.42 \pm 1.70 ^{bA}	19.75 \pm 4.27 ^{bA}
	Low	5.95 \pm 1.06 ^{aB}	1.23 \pm 0.28 ^{aB}	18.27 \pm 1.06 ^{aB}	1.46 \pm 0.06 ^{aA}	12.47 \pm 0.22 ^{aB}	31.51 \pm 1.83 ^{aB}
	Mean	6.68 \pm 0.67 ^B	0.99 \pm 0.25 ^B	14.86 \pm 1.57 ^B	1.39 \pm 0.04 ^A	10.44 \pm 0.98 ^A	25.63 \pm 2.71 ^B

307

308 **3.4 Vegetation structure and biomass**

309 Only the species *R. mangle* and *A. germinans* were found in the floristic survey carried
310 out. The DBH did not vary significantly between the topographies for either species
311 (Table 3). However, *R. mangle* had a higher DBH than *A. germinaris* at both high
312 (LSD: 139.304; $p = 0.037$) and low topographies (LSD: 131.307; $p = 0.001$). The basal
313 area (BA) and AGB did not show significant variation (Table 3). A total aboveground
314 biomass of $322.1 \pm 49.6 \text{ Mg ha}^{-1}$ was estimated.

315

316 Table 3: Summed Diameter at Breast Height (DBH; cm), Basal Area (BA; m² ha⁻¹) and Aboveground Biomass (AGB; Mg ha⁻¹) at high and low
 317 topographies in the mangrove forest of the Mojuim River estuary. Numbers represent the mean ± standard error of the mean. Lower case letters
 318 compare topographic height for each species, and upper-case letters compare species at each topographic height, using Tukey's test (p < 0.05).

Specie	Topography	N ha ⁻¹	DBH (cm)	BA (m ² ha ⁻¹)	AGB (Mg ha ⁻¹)
<i>Rhizophora</i>	High	302.4±20.5	238.8±24.9 ^{aA}	17.3±2.0 ^{aA}	219.3±25.7 ^{aA}
<i>mangle</i>	Low	310.4±37.6	283.5±45.0 ^{aA}	24.2±4.3 ^{aA}	338.7±62.9 ^{aA}
<i>Avicennia</i>	High	47.7±20.5	86.8±51.2 ^{aB}	13.8±9.2 ^{aA}	135.3±94.7 ^{aA}
<i>germinans</i>	Low	15.9±9.2	46.1±29.3 ^{aB}	11.8±8.8 ^{aA}	136.0±108.3 ^{aA}
Total	High	350.2±18.4	325.6±33.6 ^a	31.1±7.5 ^a	304.5±99.8 ^a
	Low	346.2±41.0	296.0±23.7 ^a	30.0±4.1 ^a	330.8±60.4 ^a

319 The equations for biomass estimates (AGB) were: *R. mangle* = 0.1282*DBH^{2.6}; *A. germinans* = 0.14*DBH^{2.4}; and Total = 0.168*ρ*DBH^{2.47}, where ρ_{*R. mangle*} = 0.87; ρ_{*A. germinans*}
 320 = 0.72 (Howard et al., 2014).

321

322 **3.5 Drivers of greenhouse gas fluxes**

323 In the rainy season, CO₂ efflux was correlated with T_{air} (Pearson = 0.23, p = 0.03), RH
324 (Pearson = -0.32, p < 0.00) and T_s (Pearson = 0.21, p = 0.04) only at the low
325 topography. In the dry season CO₂ flux was correlated with T_s (Pearson = 0.39, p <
326 0.00) at the low topography. The dry season was the period in which we found the
327 greatest amount of significant correlations between CO₂ efflux and soil chemical
328 parameters, while the C:N ratio, OM, and Eh were correlated with CO₂ efflux in both
329 seasons (Table 4). The negative correlation between T_C, N_T, C/N, and OM, along with
330 the positive correlation of N_{mic} with soil CO₂ flux, in the dry period, indicates that
331 microbial activity is a decisive factor for CO₂ efflux (Table 4). Soil moisture in the
332 Mojuim River mangrove forest negatively influenced CO₂ flux in both seasons (Table
333 4). However, soil moisture was not correlated with CH₄ flux. No significant correlations
334 were found between CH₄ efflux and the chemical properties of the soil in the mangrove
335 of the Mojuim River estuary (Table 4). However, more detailed studies on CH₄ efflux
336 and on its relationship with methanotrophic bacteria and abiotic factors (mainly
337 ammonia and sulfate) are needed due to the average flux of 4.70 mg C m⁻² h⁻¹ and the
338 extreme monthly and seasonal variations.

339

340 Table 4. Correlation coefficient (Pearson) of CO₂ and CH₄ fluxes with chemical parameters of the soil in a mangrove area in the Mojuim River
 341 estuary.

Gas Flux (g m ⁻² d ⁻¹)	Season	T _C (g kg ⁻¹)	T _N (g kg ⁻¹)	C _{mic} (mg kg ⁻¹)	N _{mic} (mg kg ⁻¹)	C/N	OM (g kg ⁻¹)	Sal (ppt)	Eh (mV)	pH	Moisture (%)
CO ₂	Dry	-0.68**	-0.59*	0.18 ^{NS}	0.61**	-0.66**	-0.67**	-0.07 ^{NS}	0.51*	0.21 ^{NS}	-0.49*
	Rainy	-0.44 ^{NS}	-0.20 ^{NS}	-0.15 ^{NS}	-0.32 ^{NS}	-0.50*	-0.63**	-0.54*	0.53*	0.47 ^{NS}	-0.54*
	Annual	-0.50**	-0.35*	-0.18 ^{NS}	0.00 ^{NS}	-0.53**	-0.48**	-0.30 ^{NS}	0.39*	0.23 ^{NS}	-0.56**
CH ₄	Dry	0.30 ^{NS}	0.07 ^{NS}	-0.14 ^{NS}	-0.24 ^{NS}	0.34 ^{NS}	0.02 ^{NS}	-0.04 ^{NS}	-0.38 ^{NS}	0.26 ^{NS}	0.26 ^{NS}
	Rainy	0.05 ^{NS}	-0.09 ^{NS}	0.44 ^{NS}	-0.27 ^{NS}	0.09 ^{NS}	-0.11 ^{NS}	-0.04 ^{NS}	-0.13 ^{NS}	-0.07 ^{NS}	0.04 ^{NS}
	Annual	0.04 ^{NS}	-0.10 ^{NS}	-0.01 ^{NS}	-0.18 ^{NS}	0.08 ^{NS}	-0.01 ^{NS}	-0.17 ^{NS}	-0.21 ^{NS}	-0.08 ^{NS}	0.02 ^{NS}

342 Total Carbon (T_C; g kg⁻¹); Total Nitrogen (T_N; g kg⁻¹); Microbial Carbon (C_{mic}, g kg⁻¹); Microbial Nitrogen (N_{mic}, g kg⁻¹); Carbon and Nitrogen
 343 ratio (C/N); Organic Matter (OM; g kg⁻¹); Salinity (Sal; ppt); Redox Potential (Eh; mV); Soil Moisture (Moisture, %).

344 NS= not significant; * significant effects at p ≤ 0.05; ** significant effects at p ≤ 0.01

345

346 4 Discussion

347 4.1 Carbon dioxide and methane flux

348 It is important to consider that the year under study was rainier in the dry season (2017)
349 and less rainy in the wet season (2018) when the climatological average is concerned
350 (1981-2010) (Figure 3). Perhaps this variation is related to the effects of global climate
351 changes. Under these conditions, negative and positive ~~flows-fluxes~~ of the two
352 greenhouse gases were found (negative values represent gas consumption). ~~Under these~~
353 ~~conditions, the CO₂ flux from the mangrove soil ranged from -5.06 to 68.96 g CO₂ m⁻²~~
354 ~~d⁻¹ (mean 6.66 g CO₂ m⁻² d⁻¹), while the CH₄ flux ranged from -5.07 to 11.08 g CH₄ m⁻²~~
355 ~~d⁻¹ (mean 0.13 g CH₄ m⁻² d⁻¹), resulting in a total carbon rate of 1.92 g C m⁻² d⁻¹ or 7.00~~
356 ~~Mg C ha⁻¹ y⁻¹ (Figure 2).~~ The negative CO₂ flux is apparently a consequence of the
357 increased CO₂ solubility in tidal waters or of the increased sulfate reduction, as
358 described in the literature (Borges et al., 2018; Chowdhury et al., 2018; Nóbrega et al.,
359 2016). Fluctuations in redox potential altered the availability of the terminal electron
360 acceptor and donor, and the forces of recovery of their concentrations in the soil, such
361 that a disproportionate release of CO₂ can result from the alternative anaerobic
362 degradation processes such as sulfate and iron reduction (Chowdhury et al., 2018). The
363 soil carbon flux in the mangrove area in the Amazon region was within the range of
364 findings for other tropical mangrove areas (2.57-6 to 11.00 g CO₂ m⁻² d⁻¹; Shiau and
365 Chiu, 2020). However, the mean flux of 6.2 mmol CO₂ m⁻² h⁻¹ recorded in this
366 Amazonian mangrove was much higher than the mean efflux of 2.9 mmol CO₂ m⁻² h⁻¹
367 recorded in 75 mangroves during low tide periods (Alongi, 2009).

368 An emission of 0.010 Tg CH₄ y⁻¹, 0.64 g CH₄ m⁻² d⁻¹ (Rosentreter et al., 2018a), or 26.7
369 mg CH₄ m⁻² h⁻¹ has been reported for tropical latitudes (0 and 5°). In our study, the
370 monthly average of CH₄ flux was higher at the low (7.3 ± 8.0 mg CH₄ m⁻² h⁻¹) than at
371 the high topography (0.9 ± 0.6 mg C m⁻² h⁻¹), resulting in 0.13 g CH₄ m⁻² d⁻¹ or 0.48-5
372 Mg CH₄ ha⁻¹ y⁻¹ (Figure 2). Therefore, the CH₄-C fluxes from the mangrove soil in the
373 Mojuim River estuary were much lower than expected. It is known that there is a
374 microbial functional module for CH₄ production and consumption (Xu et al., 2015) and
375 diffusibility of CH₄ (Sihi et al., 2018), and this module considers three key mechanisms:
376 acetoclastic methanogenesis (acetate production), hydrogenotrophic methanogenesis (H₂
377 and CO₂ production), and aerobic methanotrophy (CH₄ oxidation and O₂ reduction).
378 The average emission from the soil of 8.4 mmol CH₄ m⁻² d⁻¹ was well below the fluxes

379 recorded in the Bay of Bengal, with $18.4 \text{ mmol CH}_4 \text{ m}^{-2} \text{ d}^{-1}$ (Biswas et al., 2007). In the
380 Amazonian mangrove studied the mean annual carbon equivalent efflux was 429.6 mg
381 $\text{CO}_2\text{-eq m}^{-2} \text{ h}^{-1}$. This value ~~is insignificant compared to the projected is 0.00004% of the~~
382 erosion losses of $103.5 \text{ Tg CO}_2\text{-eq ha}^{-1} \text{ y}^{-1}$ ~~projected~~ for the next century in tropical
383 mangrove forests (Adame et al., 2021). These higher CO_2 flux concomitantly with
384 lower CH_4 flux in this Amazonian estuary are probably a consequence of changes in the
385 rainfall pattern already underway, where the dry season was wetter and the rainy season
386 drier when compared to the climatological normal. The most recent estimate between
387 latitude 0° to 23.5° S shows an emission of $2.3 \text{ g CO}_2 \text{ m}^{-2} \text{ d}^{-1}$ (Rosentreter et al., 2018b).
388 However, the efflux in the mangrove of the Mojuim River estuary was $6.7 \text{ g CO}_2 \text{ m}^{-2} \text{ d}^{-1}$
389 ¹. For the same latitudinal range, Rosentreter et al. (2018c) estimated an emission of
390 $0.64 \text{ g CH}_4 \text{ m}^{-2} \text{ d}^{-1}$, and we found an efflux of $0.13 \text{ g CH}_4 \text{ m}^{-2} \text{ d}^{-1}$.

391 4.2 Drivers of greenhouse gas fluxes

392 Mangrove areas are periodically flooded, with a larger flood volume during the syzygy
393 tides, especially in the rainy season. The hydrological condition of the soil is determined
394 by the microtopography and can regulate the respiration of microorganisms (aerobic or
395 anaerobic), being a decisive factor in controlling the CO_2 efflux (Dai et al., 2012;
396 Davidson et al., 2000; Ehrenfeld, 1995). ~~In the two climatic periods of the year, the high~~
397 ~~topography produced more CO_2 ($7.869 \pm 1.873 \text{ g CO}_2 \text{ m}^{-2} \text{ d}^{-1}$) than the low topography~~
398 ~~($5.212 \pm 1.225 \text{ g CO}_2 \text{ m}^{-2} \text{ d}^{-1}$) (Figure 2; SI 1).~~ No significant influence on CO_2 flux was
399 observed due to the low variation in high tide level throughout the year (0.19 m) (Figure
400 2), although it was numerically higher at the high topography. However, tidal height
401 and the rainy season resulted in a higher CO_2 flux (rate high/low = 1.7) at the high
402 topography (~~$7.858\text{-}86 \pm 0.039\text{-}04 \text{ g CO}_2 \text{ m}^{-2} \text{ d}^{-1}$~~) than at the low topography ($4.734 \pm$
403 $0.335\text{-}34 \text{ g CO}_2 \text{ m}^{-2} \text{ d}^{-1}$) (Figure 2; SI 1). This result ~~is because may be due to~~ the root
404 systems of most flood-tolerant plants remain~~ing~~ active when flooded (Angelov et al.,
405 1996). Still, the high topography has longer flood-free periods, which only happens
406 when the tides are syzygy or when the rains are torrential.

407 CO_2 efflux was higher in the high topography than in the low topography in the rainy
408 season (when soils are more subject to inundation), i.e., 39.8% lower in the forest soil
409 exposed to the atmosphere for less time. Measurements performed on 62 mangrove
410 forest soils showed an average flux of $2.87 \text{ mmol CO}_2 \text{ m}^{-2} \text{ h}^{-1}$ when the soil was
411 exposed to the atmosphere, while 75 results on flooded mangrove forest soils showed an

412 average emission of $2.06 \text{ mmol CO}_2 \text{ m}^{-2} \text{ h}^{-1}$ (Alongi, 2007, 2009), i.e., 28.2% less than
413 for the dry soil. This reflects the increased facility gases have for molecular diffusion
414 than fluids, and the increased surface area available for aerobic respiration and chemical
415 oxidation during air exposure (Chen et al., 2010). Some studies attribute this variation
416 to the temperature of the soil when it is exposed to tropical air (Alongi, 2009), which
417 increases the export of dissolved inorganic carbon (Maher et al., 2018). However,
418 although despite the lack of significant variation in soil temperature between
419 topographies at each time of year (Figure 4b), there was a positive correlation (Pearson
420 $= 0.15$, $p = 0.05$) between CO_2 efflux and soil temperature at the low topography.

421 Some studies show that CH_4 efflux is a consequence of the seasonal temperature
422 variation in mangrove forest under temperate/monsoon climates (Chauhan et al., 2015;
423 Purvaja and Ramesh, 2001; Whalen, 2005). However, in your study CH_4 efflux was
424 correlated with T_a (Pearson $= -0.33$, $p < 0.00$) and RH (Pearson $= 0.28$, $p = 0.01$) only
425 in the dry season and at the low topography. The results show that the physical
426 parameters do not affect the fluxes in a standardized way, and their greater or lesser
427 influence depends on the topography and seasonality.

428 A compilation of several studies showed that the total CH_4 emissions from the soil in a
429 mangrove ecosystem range from 0 to $23.68 \text{ mg C m}^{-2} \text{ h}^{-1}$ (Shiau and Chiu, 2020), and
430 our study showed a range of -0.01 to $31.88 \text{ mg C m}^{-2} \text{ h}^{-1}$ (mean of $4.70 \pm 5.00 \text{ mg C m}^{-2}$
431 h^{-1}). The monthly CH_4 fluxes were generally higher at the low ($0.232 \pm 0.256 \text{ g CH}_4 \text{ m}^{-2}$
432 d^{-1}) than at the high ($0.026 \pm 0.018 \text{ g CH}_4 \text{ m}^{-2} \text{ d}^{-1}$) topography, especially during the
433 rainy season when the tides were higher (Figure 2). Only in the dry season was there a
434 significantly higher production at the low than at the high topography (Figure 2; SI 1).
435 The low topography produced $0.0249 \text{ g C m}^{-2} \text{ h}^{-1}$ more to the atmosphere in the rainy
436 season than in the dry season (Figure 2), and a similar seasonal pattern was recorded in
437 other studies (Cameron et al., 2021).

438 The mangrove soil in the Mojuim River estuary is rich in silt and clay (Table 1), which
439 reduces sediment porosity and fosters the formation and maintenance of anoxic
440 conditions (Dutta et al., 2013). In addition, the lack of oxygen in the flooded mangrove
441 soil favors microbial processes such as denitrification, sulfate reduction,
442 methanogenesis, and redox reactions (Alongi and Christoffersen, 1992). A significant
443 amount of CH_4 produced in wetlands is dissolved in the pore water due to high pressure,

444 causing supersaturation, which allows CH₄ to be released by diffusion from the
445 sediment to the atmosphere and by boiling through the formation of bubbles.

446 Studies show that the CO₂ flux tends to be lower with high soil saturation (Chanda et
447 al., 2014; Kristensen et al., 2008). A total of 395 Mg C ha⁻¹ was found at the soil surface
448 (0.15 m) in the mangrove of the Mojuim River estuary, which was slightly higher than
449 the 340 Mg C ha⁻¹ found in other mangroves in the Amazon (Kauffman et al., 2018),
450 however being significantly 1.8 times greater at the low topography (Table 2). The finer
451 soil texture at the low topography (Table 1) reduces groundwater drainage which
452 facilitates the accumulation of C in the soil (Schmidt et al., 2011).

453 **4.3 Mangrove biomass**

454 Only the species *R. mangle* and *A. germinans* were found in the floristic survey carried
455 out, which is aligned with the results of other studies in the same region (Menezes et al.,
456 2008). Thus, the variations found in the flux between the topographies in the Mojuim
457 River estuary are not related to the mangrove forest structure, because there was no
458 difference in the aboveground biomass. Since there was no difference in the species
459 composition, the belowground biomass is not expected to differ either (Table 3).

460 Assuming that the amount of carbon stored is ~~0.42.0%~~ of the total biomass (Sahu and
461 Kathiresan, 2019), the mangrove forest biomass of the Mojuim River estuary stores
462 127.9 and 138.9 Mg C ha⁻¹ at the high and low topographies, respectively. This result is
463 ~~lower than well below~~ the 507.8 Mg C ha⁻¹ estimated for Brazilian mangroves
464 (Hamilton and Friess, 2018), but are near the 103.7 Mg C ha⁻¹ estimated for a mangrove
465 at Guará's island (Salum et al., 2020), 108.4 Mg C ha⁻¹ for the Bragantina region
466 (Gardunho, 2017), and 132.3 Mg C ha⁻¹ in French Guiana (Fromard et al., 1998). Thus,
467 ~~the biomass found in the Mojuim estuary does not differ from the biomass found in~~
468 ~~other Amazonian mangroves, despite being much lower than that found in other~~
469 ~~Brazilian mangroves.~~ The estimated primary production for tropical mangrove forests is
470 218 ± 72 Tg C y⁻¹ (Bouillon et al., 2008).

471 **4.4 Biogeochemical parameters**

472 During the seasonal and annual periods, CH₄ efflux was not significantly correlated
473 with chemical parameters (Table 5), which is similar to the observed in another study
474 (Chen et al., 2010). Flooded soils present reduced gas diffusion rates, which directly
475 affects the physiological state and activity of microbes, by limiting the supply of the

476 dominant electron acceptors (e.g., oxygen), and gases (e.g., CH₄) (Blagodatsky and
477 Smith, 2012). The importance of soil ~~can be reflected in bacterial moisture was evident~~
478 ~~in the richness and diversity of bacterial communities in a study that~~ compared the ~~o~~
479 ~~different~~ pore spaces filled with water (Banerjee et al., 2016). ~~Furthermore, sulfate~~
480 ~~reduction in flooded soils (another pathway of organic matter metabolism) is dependent~~
481 ~~on the redox potential of the soil. However, no sulfate reduction occurs when the redox~~
482 ~~potential has values are above -150 mv (Connell and Patrick, 1968). In our study, Eh~~
483 ~~was above 36.0 mV indicating that sulfate reduction probably did not influence the OM~~
484 ~~metabolism.~~

Código de campo alterado

485 On the other hand, increasing soil moisture provides the microorganisms with essential
486 substrates such as ammonium, nitrate, and soluble organic carbon, and increases gas
487 diffusion rates in the water (Blagodatsky and Smith, 2012). Biologically available
488 nitrogen often limit marine productivity (Bertics et al., 2010), and thus can affect CO₂
489 fluxes to the atmosphere. However, a mangrove fertilization experiment showed that
490 CH₄ emission rates were not affected by N addition (Kreuzwieser et al., 2003). A higher
491 concentration of C_{mic} and N_{mic} in the dry period (Table 2), both in the high and low
492 topographies, indicated that microorganisms are more active when the soil spends more
493 time aerated in the dry period (Table 2), ~~period-time~~ when only the high tides produce
494 anoxia in the mangrove soil mainly in the low topography. Under reduced oxygen
495 conditions, in a laboratory incubated mangrove soil, the addition of nitrogen resulted in
496 a significant increase in the microbial metabolic quotient, showing no concomitant
497 change in microbial respiration, which was explained by a decrease in microbial
498 biomass (Craig et al., 2021).

499 The high OM concentration at the two topographic ~~heights-locations~~ (Table 2), at the
500 two seasons studied, and the respective negative correlation with CO₂ flux (Table 5)
501 confirm the importance of microbial activity in mangrove soils (Gao et al., 2020). Also,
502 CH₄ produced in flooded soils can be converted mainly to CO₂ by the anaerobic
503 oxidation of CH₄ (Boetius et al., 2000; Milucka et al., 2015; Xu et al., 2015) which may
504 contribute to the higher CO₂ efflux in the Mojuim River estuary compared to other
505 tropical mangroves (Rosentreter et al., 2018b). The belowground C stock is considered
506 the largest C reservoir in a mangrove ecosystem, and it results from the low OM
507 decomposition rate due to flooding (Marchand, 2017).

508 The higher water salinity influenced by the tidal movement in the dry season (Table 1)
509 seems to result in a lower CH₄ flux at the low topography (Dutta et al., 2013; Lekphet et
510 al., 2005; Shiau and Chiu, 2020). ~~Sulfate-High (SO₄²⁻ concentration in the marine~~
511 ~~sediments inhibits methane formation due to competition between SO₄²⁻ reduction and~~
512 ~~methanogenic fermentation, as) in the brine affects the competition between SO₄²⁻~~
513 ~~reduction and methanogenic fermentation, as~~ sulfate-reducing bacteria are more
514 efficient at using hydrogen than methanotrophic bacteria (Abram and Nedwell, 1978;
515 Kristjansson et al., 1982), a key factor fostering reduced CH₄ emissions. At high SO₄²⁻
516 concentrations methanotrophic bacteria use CH₄ as an energy source and oxidize it to
517 CO₂ (Coyne, 1999; Segarra et al., 2015), increasing the efflux of CO₂ and reduced CH₄
518 (Megonigal and Schlesinger, 2002; Roslev and King, 1996). This may explain the high
519 CO₂ and low CH₄ efflux found throughout the year at the high and, especially, at the
520 low topographies (Figure 3).

521 Studies in coastal ecosystems in Taiwan have reported that methanotrophic bacteria can
522 be sensitive to soil pH, and reported an optimal growth at pH ranging from 6.5 to 7.5
523 (Shiau et al., 2018). The higher soil acidity in the Mojuim River wetland (Table 1) may
524 be inhibiting the activity of methanogenic bacteria by increasing the population of
525 methanotrophic bacteria, which are efficient in CH₄ consumption (Chen et al., 2010;
526 Hegde et al., 2003; Shiau and Chiu, 2020). In addition, the pneumatophores present in
527 *R. mangle* increase soil aeration and reduce CH₄ emissions (Allen et al., 2011; He et al.,
528 2019). Spatial differences (topography) in CH₄ emissions in the soil can be attributed to
529 substrate heterogeneity, salinity, and the abundance of methanogenic and
530 methanotrophic bacteria (Gao et al., 2020). ~~The high Eh values found in both~~
531 ~~topographies, mainly in the dry period (Table 1), hinder CH₄ emission. Soil Eh above~~
532 ~~150 mV has been considered limiting for CH₄ production (Yang and Chang, 1998).~~
533 Increases in CH₄ efflux with reduced salinity were found as a consequence of intense
534 oxidation or reduced competition from the more energetically efficient SO₄²⁻ and NO₃³⁻
535 reducing bacteria when compared to the methanogenic bacteria (Biswas et al., 2007).
536 This fact can be observed in the CH₄ efflux in the mangrove of the Mojuim River,
537 because there was an increased CH₄ production especially in the low topography in the
538 rainy season (Figure 3), when water salinity is reduced (Table 1) due to the increased
539 precipitation. However, we did not find a correlation between CH₄ efflux and salinity,
540 as previously reported (Purvaja and Ramesh, 2001)

541 5 Conclusions

542 ~~The most recent estimate between latitude 0° to 23.5° S shows an emission of 2.3 g CO₂~~
543 ~~m⁻² d⁻¹ (Rosentreter et al., 2018b). However, the efflux in the mangrove of the Mojuim~~
544 ~~River estuary was 6.7 g CO₂ m⁻² d⁻¹. For the same latitudinal range, Rosentreter et al.~~
545 ~~(2018c) estimated an emission of 0.64 g CH₄ m⁻² d⁻¹, and we found an efflux of 0.13 g~~
546 ~~CH₄ m⁻² d⁻¹. Seasonality was important for CH₄ efflux but did not influence CO₂ efflux.~~
547 Seasonality was important for CH₄ efflux but did not influence CO₂ efflux. The
548 differences in fluxes may be an effect of global climate changes on the terrestrial
549 biogeochemistry at the plant-soil-atmosphere interface, as indicated by the deviation in
550 precipitation values from the climatology normal, making it necessary to extend this
551 study for more years. Using the factor of 23 to convert the global warming potential of
552 CH₄ to CO₂ (IPCC, 2001), the CO₂ equivalent emission was 35.4 Mg CO₂-eq ha⁻¹ yr⁻¹.
553 Over a 100-year time period, a radiative forcing due to the continuous emission of 0.05
554 kg CH₄ m⁻² y⁻¹ found in this study, would be offset if CO₂ sequestration rates were 2.16
555 kg CO₂ m⁻² y⁻¹ (Neubauer and Megonigal, 2015).

556 Microtopography should be considered when determining the efflux of CO₂ and CH₄ in
557 mangrove forests in an Amazon estuary. The low topography in the mangrove forest of
558 Mojuim River had a higher concentration of organic carbon in the soil. However, it did
559 not produce a higher CO₂ efflux because it was negatively influenced by soil moisture,
560 which was indifferent to CH₄ efflux. MO, C/N ratio, and Eh were critical in soil
561 microbial activity, which resulted in a variation in CO₂ flux during the year and
562 seasonal periods. Thus, the physicochemical properties of the soil are important for CO₂
563 flux, especially in the rainy season. Still, they did not influence CH₄ fluxes.

564 *Data availability:* The data used in this article belong to the doctoral thesis of Saul
565 Castellón, within the Postgraduate Program in Environmental Sciences, at the Federal
566 University of Pará. Access to the data can be requested from Dr. Castellón
567 (saulmarz22@gmail.com), which holds the set of all data used in this paper.

568 *Author contributions:* SEMC and JHC designed the study and wrote the article with the
569 help of JFB, MR, MLR, and CN. JFB assisted in the field experiment. MR provided
570 logistical support in field activities.

571 *Competing interests:* The authors declare that they have no conflict of interest

572 *Acknowledgements:* The authors are grateful to the Program of Alliances for Education
573 and Training of the Organization of the American States and to Coimbra Group of
574 Brazilian Universities, for the financial support, as well as to Paulo Sarmento for the
575 assistance at laboratory analysis, and to Maridalva Ribeiro and Lucivaldo da Silva for
576 the fieldwork assistance. Furthermore, the authors would like to thank the Laboratory of
577 Biogeochemical Cycles (Geosciences Institute, Federal University of Pará) for the
578 equipment provided for this research.

579 **6 References**

580 Abram, J. W. and Nedwell, D. B.: Inhibition of methanogenesis by sulphate reducing
581 bacteria competing for transferred hydrogen, *Arch. Microbiol.*, 117(1), 89–92,
582 doi:10.1007/BF00689356, 1978.

583 Adame, M. F., Connolly, R. M., Turschwell, M. P., Lovelock, C. E., Fatoyinbo, T.,
584 Lagomasino, D., Goldberg, L. A., Holdorf, J., Friess, D. A., Sasmito, S. D., Sanderman,
585 J., Sievers, M., Buelow, C., Kauffman, J. B., Bryan-Brown, D. and Brown, C. J.: Future
586 carbon emissions from global mangrove forest loss, *Glob. Chang. Biol.*, 27(12), 2856–
587 2866, doi:10.1111/gcb.15571, 2021.

588 Allen, D., Dalal, R. C., Rennenberg, H. and Schmidt, S.: Seasonal variation in nitrous
589 oxide and methane emissions from subtropical estuary and coastal mangrove sediments,
590 Australia, *Plant Biol.*, 13(1), 126–133, doi:10.1111/j.1438-8677.2010.00331.x, 2011.

591 Almeida, R. F. de, Mikhael, J. E. R., Franco, F. O., Santana, L. M. F. and Wendling, B.:
592 Measuring the labile and recalcitrant pools of carbon and nitrogen in forested and
593 agricultural soils: A study under tropical conditions, *Forests*, 10(7), 544,
594 doi:10.3390/f10070544, 2019.

595 Alongi, D. M.: The contribution of mangrove ecosystems to global carbon cycling and
596 greenhouse gas emissions, in *Greenhouse gas and carbon balances in mangrove coastal
597 ecosystems*, edited by Y. Tateda, R. Upstill-Goddard, T. Goreau, D. M. Alongi, A.
598 Nose, E. Kristensen, and G. Wattayakorn, pp. 1–10, Gendai Tosho, Kanagawa, Japan.,
599 2007.

600 Alongi, D. M.: *The Energetics of Mangrove Forests*, Springer Netherlands, Dordrecht.,
601 2009.

602 Alongi, D. M. and Christoffersen, P.: Benthic infauna and organism-sediment relations

603 in a shallow, tropical coastal area: influence of outwelled mangrove detritus and
604 physical disturbance, *Mar. Ecol. Prog. Ser.*, 81(3), 229–245, doi:10.3354/meps081229,
605 1992.

606 Alongi, D. M. and Mukhopadhyay, S. K.: Contribution of mangroves to coastal carbon
607 cycling in low latitude seas, *Agric. For. Meteorol.*, 213, 266–272,
608 doi:10.1016/j.agrformet.2014.10.005, 2015.

609 Angelov, M. N., Sung, S. J. S., Doong, R. Lou, Harms, W. R., Kormanik, P. P. and
610 Black, C. C.: Long-and short-term flooding effects on survival and sink-source
611 relationships of swamp-adapted tree species, *Tree Physiol.*, 16(4), 477–484,
612 doi:10.1093/treephys/16.5.477, 1996.

613 Araujo, A. S. F. de: Is the microwave irradiation a suitable method for measuring soil
614 microbial biomass?, *Rev. Environ. Sci. Biotechnol.*, 9(4), 317–321,
615 doi:10.1007/s11157-010-9210-y, 2010.

616 Banerjee, S., Helgason, B., Wang, L., Winsley, T., Ferrari, B. C. and Siciliano, S. D.:
617 Legacy effects of soil moisture on microbial community structure and N₂O emissions,
618 *Soil Biol. Biochem.*, 95, 40–50, doi:10.1016/j.soilbio.2015.12.004, 2016.

619 Bastviken, D., Tranvik, L. J., Downing, J. A., Crill, P. M. and Enrich-Prast, A.:
620 Freshwater Methane Emissions Offset the Continental Carbon Sink, *Science* (80-.),
621 331(6013), 50–50, doi:10.1126/science.1196808, 2011.

622 Bauza, J. F., Morell, J. M. and Corredor, J. E.: Biogeochemistry of Nitrous Oxide
623 Production in the Red Mangrove (*Rhizophora mangle*) Forest Sediments, *Estuar. Coast.*
624 *Shelf Sci.*, 55(5), 697–704, doi:10.1006/ECSS.2001.0913, 2002.

625 Bertics, V. J., Sohm, J. A., Treude, T., Chow, C. E. T., Capone, D. G., Fuhrman, J. A.
626 and Ziebis, W.: Burrowing deeper into benthic nitrogen cycling: The impact of
627 Bioturbation on nitrogen fixation coupled to sulfate reduction, *Mar. Ecol. Prog. Ser.*,
628 409, 1–15, doi:10.3354/meps08639, 2010.

629 Biswas, H., Mukhopadhyay, S. K., Sen, S. and Jana, T. K.: Spatial and temporal
630 patterns of methane dynamics in the tropical mangrove dominated estuary, NE coast of
631 Bay of Bengal, India, *J. Mar. Syst.*, 68(1–2), 55–64, doi:10.1016/j.jmarsys.2006.11.001,
632 2007.

633 Blagodatsky, S. and Smith, P.: Soil physics meets soil biology: Towards better

634 mechanistic prediction of greenhouse gas emissions from soil, *Soil Biol. Biochem.*, 47,
635 78–92, doi:10.1016/J.SOILBIO.2011.12.015, 2012.

636 Boetius, A., Ravenschlag, K., Schubert, C. J., Rickert, D., Widdel, F., Gleseke, A.,
637 Amann, R., Jørgensen, B. B., Witte, U. and Pfannkuche, O.: A marine microbial
638 consortium apparently mediating anaerobic oxidation methane, *Nature*, 407(6804), 623–
639 626, doi:10.1038/35036572, 2000.

640 Borges, A. V., Abril, G., Darchambeau, F., Teodoru, C. R., Deborde, J., Vidal, L. O.,
641 Lambert, T. and Bouillon, S.: Divergent biophysical controls of aquatic CO₂ and CH₄
642 in the World's two largest rivers, *Sci. Rep.*, 5, doi:10.1038/srep15614, 2015.

643 Borges, A. V., Abril, G. and Bouillon, S.: Carbon dynamics and CO₂ and CH₄
644 outgassing in the Mekong delta, *Biogeosciences*, 15(4), 1093–1114, doi:10.5194/bg-15-
645 1093-2018, 2018.

646 Bouillon, S., Borges, A. V., Castañeda-Moya, E., Diele, K., Dittmar, T., Duke, N. C.,
647 Kristensen, E., Lee, S. Y., Marchand, C., Middelburg, J. J., Rivera-Monroy, V. H.,
648 Smith, T. J. and Twilley, R. R.: Mangrove production and carbon sinks: A revision of
649 global budget estimates, *Global Biogeochem. Cycles*, 22(2), 1–12,
650 doi:10.1029/2007GB003052, 2008.

651 Brookes, P. C., Landman, A., Pruden, G. and Jenkinson, D. S.: Chloroform fumigation
652 and the release of soil nitrogen: A rapid direct extraction method to measure microbial
653 biomass nitrogen in soil, *Soil Biol. Biochem.*, 17(6), 837–842, doi:10.1016/0038-
654 0717(85)90144-0, 1985.

655 Cameron, C., Hutley, L. B., Munksgaard, N. C., Phan, S., Aung, T., Thinn, T., Aye, W.
656 M. and Lovelock, C. E.: Impact of an extreme monsoon on CO₂ and CH₄ fluxes from
657 mangrove soils of the Ayeyarwady Delta, Myanmar, *Sci. Total Environ.*, 760, 143422,
658 doi:10.1016/j.scitotenv.2020.143422, 2021.

659 Castillo, J. A. A., Apan, A. A., Maraseni, T. N. and Salmo, S. G.: Soil greenhouse gas
660 fluxes in tropical mangrove forests and in land uses on deforested mangrove lands,
661 *Catena*, 159, 60–69, doi:10.1016/j.catena.2017.08.005, 2017.

662 Chanda, A., Akhand, A., Manna, S., Dutta, S., Das, I., Hazra, S., Rao, K. H. and
663 Dadhwal, V. K.: Measuring daytime CO₂ fluxes from the inter-tidal mangrove soils of
664 Indian Sundarbans, *Environ. Earth Sci.*, 72(2), 417–427, doi:10.1007/s12665-013-2962-

665 2, 2014.

666 Chauhan, R., Datta, A., Ramanathan, A. and Adhya, T. K.: Factors influencing spatio-
667 temporal variation of methane and nitrous oxide emission from a tropical mangrove of
668 eastern coast of India, *Atmos. Environ.*, 107, 95–106,
669 doi:10.1016/j.atmosenv.2015.02.006, 2015.

670 Chen, G. C., Tam, N. F. Y. and Ye, Y.: Spatial and seasonal variations of atmospheric
671 N₂O and CO₂ fluxes from a subtropical mangrove swamp and their relationships with
672 soil characteristics, *Soil Biol. Biochem.*, 48, 175–181,
673 doi:10.1016/j.soilbio.2012.01.029, 2012.

674 Chen, G. C., Ulumuddin, Y. I., Pramudji, S., Chen, S. Y., Chen, B., Ye, Y., Ou, D. Y.,
675 Ma, Z. Y., Huang, H. and Wang, J. K.: Rich soil carbon and nitrogen but low
676 atmospheric greenhouse gas fluxes from North Sulawesi mangrove swamps in
677 Indonesia, *Sci. Total Environ.*, 487(1), 91–96, doi:10.1016/j.scitotenv.2014.03.140,
678 2014.

679 Chen, G. C. C., Tam, N. F. Y. F. Y. and Ye, Y.: Summer fluxes of atmospheric
680 greenhouse gases N₂O, CH₄ and CO₂ from mangrove soil in South China, *Sci. Total*
681 *Environ.*, 408(13), 2761–2767, doi:10.1016/j.scitotenv.2010.03.007, 2010.

682 Chowdhury, T. R., Bramer, L., Hoyt, D. W., Kim, Y. M., Metz, T. O., McCue, L. A.,
683 Diefenderfer, H. L., Jansson, J. K. and Bailey, V.: Temporal dynamics of CO₂ and CH₄
684 loss potentials in response to rapid hydrological shifts in tidal freshwater wetland soils,
685 *Ecol. Eng.*, 114, 104–114, doi:10.1016/j.ecoleng.2017.06.041, 2018.

686 Chuang, P. C., Young, M. B., Dale, A. W., Miller, L. G., Herrera-Silveira, J. A. and
687 Paytan, A.: Methane and sulfate dynamics in sediments from mangrove-dominated
688 tropical coastal lagoons, Yucatan, Mexico, *Biogeosciences*, 13(10), 2981–3001, 2016.

689 Connell, W. E. and Patrick, W. H.: Sulfate Reduction in Soil: Effects of Redox Potential
690 and p H, *Science* (80-.), 159(3810), 86–87, doi:10.1126/science.159.3810.86, 1968.

691 Coyne, M.: *Soil Microbiology: An Exploratory Approach*, Delmar Publishers, New
692 York, NY, USA., 1999.

693 Craig, H., Antwis, R. E., Cordero, I., Ashworth, D., Robinson, C. H., Osborne, T. Z.,
694 Bardgett, R. D., Rowntree, J. K. and Simpson, L. T.: Nitrogen addition alters
695 composition, diversity, and functioning of microbial communities in mangrove soils:

696 An incubation experiment, *Soil Biol. Biochem.*, 153, 108076,
697 doi:10.1016/j.soilbio.2020.108076, 2021.

698 Dai, Z., Trettin, C. C., Li, C., Li, H., Sun, G. and Amatya, D. M.: Effect of Assessment
699 Scale on Spatial and Temporal Variations in CH₄, CO₂, and N₂O Fluxes in a Forested
700 Wetland, *Water, Air, Soil Pollut.*, 223(1), 253–265, doi:10.1007/s11270-011-0855-0,
701 2012.

702 Davidson, E. A., Verchot, L. V., Cattanio, J. H., Ackerman, I. L. and Carvalho, J. E. M.:
703 Effects of soil water content on soil respiration in forests and cattle pastures of eastern
704 Amazonia, *Biogeochemistry*, 48(1), 53–69, doi:10.1023/a:1006204113917, 2000.

705 Donato, D. C., Kauffman, J. B., Murdiyarso, D., Kurnianto, S., Stidham, M. and
706 Kanninen, M.: Mangroves among the most carbon-rich forests in the tropics, *Nat.*
707 *Geosci.*, 4(5), 293–297, doi:10.1038/ngeo1123, 2011.

708 Dutta, M. K., Chowdhury, C., Jana, T. K. and Mukhopadhyay, S. K.: Dynamics and
709 exchange fluxes of methane in the estuarine mangrove environment of the Sundarbans,
710 NE coast of India, *Atmos. Environ.*, 77, 631–639, doi:10.1016/j.atmosenv.2013.05.050,
711 2013.

712 Ehrenfeld, J. G.: Microsite differences in surface substrate characteristics in
713 *Chamaecyparis* swamps of the New Jersey Pinelands, *Wetlands*, 15(2), 183–189,
714 doi:10.1007/BF03160672, 1995.

715 El-Robrini, M., Alves, M. A. M. S., Souza Filho, P. W. M., El-Robrini M. H. S., Silva
716 Júnior, O. G. and França, C. F.: Atlas de Erosão e Progradação da zona costeira do
717 Estado do Pará – Região Amazônica: Áreas oceânica e estuarina, in *Atlas de Erosão e*
718 *Progradação da Zona Costeira Brasileira*, edited by D. Muehe, pp. 1–34, São Paulo.,
719 2006.

720 EPA, E. P. A.: *Inventory of U.S. Greenhouse Gas Emissions and Sinks: 1990–2015.*,
721 2017.

722 Fernandes, W. A. A. and Pimentel, M. A. da S.: Dinâmica da paisagem no entorno da
723 RESEX marinha de São João da Ponta/PA: utilização de métricas e geoprocessamento,
724 *Caminhos Geogr.*, 20(72), 326–344, doi:10.14393/RCG207247140, 2019.

725 Ferreira, A. S., Camargo, F. A. O. and Vidor, C.: Utilização de microondas na avaliação
726 da biomassa microbiana do solo, *Rev. Bras. Ciência do Solo*, 23(4), 991–996,

727 doi:10.1590/S0100-06831999000400026, 1999.

728 Ferreira, S. da S.: Entre marés e mangues: paisagens territorializadas por pescadores da
729 resex marinha de São João da Ponta (PA), Federal University of Pará., 2017.

730 França, C. F. de, Pimentel, M. A. D. S. and Neves, S. C. R.: Estrutura Paisagística De
731 São João Da Ponta, Nordeste Do Pará, Geogr. Ensino Pesqui., 20(1), 130–142,
732 doi:10.5902/2236499418331, 2016.

733 Frankignoulle, M.: Field measurements of air-sea CO₂ exchange, Limnol. Oceanogr.,
734 33(3), 313–322, 1988.

735 Friesen, S. D., Dunn, C. and Freeman, C.: Decomposition as a regulator of carbon
736 accretion in mangroves: a review, Ecol. Eng., 114, 173–178,
737 doi:10.1016/j.ecoleng.2017.06.069, 2018.

738 Fromard, F., Puig, H., Cadamuro, L., Marty, G., Betoulle, J. L. and Mougin, E.:
739 Structure, above-ground biomass and dynamics of mangrove ecosystems: new data
740 from French Guiana, Oecologia, 115(1), 39–53, doi:10.1007/s004420050489, 1998.

741 Gao, G. F., Zhang, X. M., Li, P. F., Simon, M., Shen, Z. J., Chen, J., Gao, C. H. and
742 Zheng, H. L.: Examining Soil Carbon Gas (CO₂, CH₄) Emissions and the Effect on
743 Functional Microbial Abundances in the Zhangjiang Estuary Mangrove Reserve, J.
744 Coast. Res., 36(1), 54–62, doi:10.2112/JCOASTRES-D-18-00107.1, 2020.

745 Gardunho, D. C. L.: Estimativas de biomassa acima do solo da floresta de mangue na
746 península de Ajuruteua, Bragança – PA, Federal University of Pará, Belém, Brazil.,
747 2017.

748 Hamilton, S. E. and Friess, D. A.: Global carbon stocks and potential emissions due to
749 mangrove deforestation from 2000 to 2012, Nat. Clim. Chang., 8(3), 240–244,
750 doi:10.1038/s41558-018-0090-4, 2018.

751 He, Y., Guan, W., Xue, D., Liu, L., Peng, C., Liao, B., Hu, J., Zhu, Q., Yang, Y., Wang,
752 X., Zhou, G., Wu, Z. and Chen, H.: Comparison of methane emissions among invasive
753 and native mangrove species in Dongzhaigang, Hainan Island, Sci. Total Environ., 697,
754 133945, doi:10.1016/j.scitotenv.2019.133945, 2019.

755 Hegde, U., Chang, T.-C. and Yang, S.-S.: Methane and carbon dioxide emissions from
756 Shan-Chu-Ku landfill site in northern Taiwan., Chemosphere, 52(8), 1275–1285,
757 doi:10.1016/S0045-6535(03)00352-7, 2003.

758 Herz, R.: Manguezais do Brasil, Instituto Oceanografico da USP/CIRM, São Paulo,
759 Brazil., 1991.

760 Howard, J., Hoyt, S., Isensee, K., Telszewski, M. and Pidgeon, E.: Coastal Blue
761 Carbon: Methods for Assessing Carbon Stocks and Emissions Factors in Mangroves,
762 Tidal Salt Marshes, and Seagrasses, edited by J. Howard, S. Hoyt, K. Isensee, M.
763 Telszewski, and E. Pidgeon, International Union for Conservation of Nature, Arlington,
764 Virginia, USA. [online] Available from:
765 http://www.cifor.org/publications/pdf_files/Books/BMurdiyarso1401.pdf (Accessed 11
766 September 2019), 2014.

767 IPCC: Climate Change 2001: Third Assessment Report of the IPCC, Cambridge., 2001.

768 Islam, K. R. and Weil, R. R.: Microwave irradiation of soil for routine measurement of
769 microbial biomass carbon, *Biol. Fertil. Soils*, 27(4), 408–416,
770 doi:10.1007/s003740050451, 1998.

771 Kalembsa, S. J. and Jenkinson, D. S.: A comparative study of titrimetric and
772 gravimetric methods for determination of organic carbon in soil, *J. Sci. Food Agric.*, 24,
773 1085–1090, 1973.

774 Kauffman, B. J., Donato, D. and Adame, M. F.: Protocolo para la medición, monitoreo
775 y reporte de la estructura, biomasa y reservas de carbono de los manglares, Bogor,
776 Indonesia., 2013.

777 Kauffman, J. B., Bernardino, A. F., Ferreira, T. O., Giovannoni, L. R., de O. Gomes, L.
778 E., Romero, D. J., Jimenez, L. C. Z. and Ruiz, F.: Carbon stocks of mangroves and salt
779 marshes of the Amazon region, Brazil, *Biol. Lett.*, 14(9), 20180208,
780 doi:10.1098/rsbl.2018.0208, 2018.

781 Kreuzwieser, J., Buchholz, J. and Rennenberg, H.: Emission of Methane and Nitrous
782 Oxide by Australian Mangrove Ecosystems, *Plant Biol.*, 5(4), 423–431, doi:10.1055/s-
783 2003-42712, 2003.

784 Kristensen, E., Bouillon, S., Dittmar, T. and Marchand, C.: Organic carbon dynamics in
785 mangrove ecosystems: A review, *Aquat. Bot.*, 89(2), 201–219,
786 doi:10.1016/J.AQUABOT.2007.12.005, 2008.

787 Kristjansson, J. K., Schönheit, P. and Thauer, R. K.: Different K_s values for hydrogen
788 of methanogenic bacteria and sulfate reducing bacteria: An explanation for the apparent

789 inhibition of methanogenesis by sulfate, *Arch. Microbiol.*, 131(3), 278–282,
790 doi:10.1007/BF00405893, 1982.

791 Lekphet, S., Nitorisavut, S. and Adsavakulchai, S.: Estimating methane emissions from
792 mangrove area in Ranong Province, Thailand, *Songklanakarin J. Sci. Technol.*, 27(1),
793 153–163 [online] Available from: <https://www.researchgate.net/publication/26473398>
794 (Accessed 29 January 2019), 2005.

795 Maher, D. T., Call, M., Santos, I. R. and Sanders, C. J.: Beyond burial: Lateral
796 exchange is a significant atmospheric carbon sink in mangrove forests, *Biol. Lett.*,
797 14(7), 1–4, doi:10.1098/rsbl.2018.0200, 2018.

798 Mahesh, P., Sreenivas, G., Rao, P. V. N. N., Dadhwal, V. K., Sai Krishna, S. V. S. S.
799 and Mallikarjun, K.: High-precision surface-level CO₂ and CH₄ using off-axis
800 integrated cavity output spectroscopy (OA-ICOS) over Shadnagar, India, *Int. J. Remote*
801 *Sens.*, 36(22), 5754–5765, doi:10.1080/01431161.2015.1104744, 2015.

802 Marchand, C.: Soil carbon stocks and burial rates along a mangrove forest
803 chronosequence (French Guiana), *For. Ecol. Manage.*, 384, 92–99,
804 doi:10.1016/j.foreco.2016.10.030, 2017.

805 McEwing, K. R., Fisher, J. P. and Zona, D.: Environmental and vegetation controls on
806 the spatial variability of CH₄ emission from wet-sedge and tussock tundra ecosystems
807 in the Arctic, *Plant Soil*, 388(1–2), 37–52, doi:10.1007/s11104-014-2377-1, 2015.

808 Megonigal, J. P. and Schlesinger, W. H.: Methane-limited methanotrophy in tidal
809 freshwater swamps, *Global Biogeochem. Cycles*, 16(4), 35-1-35–10,
810 doi:10.1029/2001GB001594, 2002.

811 Menezes, M. P. M. de, Berger, U. and Mehlig, U.: Mangrove vegetation in Amazonia :
812 a review of studies from the coast of Pará and Maranhão States , north Brazil, *Acta*
813 *Amaz.*, 38(3), 403–420, doi:10.1590/S0044-59672008000300004, 2008.

814 Milucka, J., Kirf, M., Lu, L., Krupke, A., Lam, P., Littmann, S., Kuypers, M. M. M. and
815 Schubert, C. J.: Methane oxidation coupled to oxygenic photosynthesis in anoxic
816 waters, *ISME J.*, 9(9), 1991–2002, doi:10.1038/ismej.2015.12, 2015.

817 Monz, C. A., Reuss, D. E. and Elliott, E. T.: Soil microbial biomass carbon and nitrogen
818 estimates using 2450 MHz microwave irradiation or chloroform fumigation followed by
819 direct extraction, *Agric. Ecosyst. Environ.*, 34(1–4), 55–63, doi:10.1016/0167-

820 8809(91)90093-D, 1991.

821 Neubauer, S. C. and Megonigal, J. P.: Moving Beyond Global Warming Potentials to
822 Quantify the Climatic Role of Ecosystems, *Ecosystems*, 18(6), 1000–1013,
823 doi:10.1007/S10021-015-9879-4/TABLES/2, 2015.

824 Nóbrega, G. N., Ferreira, T. O., Siqueira Neto, M., Queiroz, H. M., Artur, A. G.,
825 Mendonça, E. D. S., Silva, E. D. O. and Otero, X. L.: Edaphic factors controlling
826 summer (rainy season) greenhouse gas emissions (CO₂ and CH₄) from semiarid
827 mangrove soils (NE-Brazil), *Sci. Total Environ.*, 542, 685–693,
828 doi:10.1016/j.scitotenv.2015.10.108, 2016.

829 Norman, J. M., Kucharik, C. J., Gower, S. T., Baldocchi, D. D., Crill, P. M., Rayment,
830 M., Savage, K. and Striegl, R. G.: A comparison of six methods for measuring soil-
831 surface carbon dioxide fluxes, *J. Geophys. Res. Atmos.*, 102(D24), 28771–28777,
832 doi:10.1029/97JD01440, 1997.

833 Peel, M. C., Finlayson, B. L. and McMahon, T. A.: Updated world map of the Köppen-
834 Geiger climate classification, *Hydrol. Earth Syst. Sci.*, 11(5), 1633–1644,
835 doi:10.1002/ppp.421, 2007.

836 Poffenbarger, H. J., Needelman, B. A. and Megonigal, J. P.: Salinity Influence on
837 Methane Emissions from Tidal Marshes, *Wetlands*, 31(5), 831–842,
838 doi:10.1007/s13157-011-0197-0, 2011.

839 Prost, M. T., Mendes, A. C., Faure, J. F., Berredo, J. F., Sales, M. E. ., Furtado, L. G.,
840 Santana, M. G., Silva, C. A., Nascimento, I. ., Gorayeb, I., Secco, M. F. and Luz, L.:
841 Manguezais e estuários da costa paraense: exemplo de estudo multidisciplinar integrado
842 (Marapanim e São Caetano de Odivelas), in *Ecosystemas Costeiros: Impactos e Gestão*
843 *Ambiental*, edited by M. T. Prost and A. Mendes, pp. 25–52, FUNTEC and Paraense
844 Museum “Emílio Goeldi,” Belém, Brazil., 2001.

845 Purvaja, R. and Ramesh, R.: Natural and Anthropogenic Methane Emission from
846 Coastal Wetlands of South India, *Environ. Manage.*, 27(4), 547–557,
847 doi:10.1007/s002670010169, 2001.

848 Purvaja, R., Ramesh, R. and Frenzel, P.: Plant-mediated methane emission from an
849 Indian mangrove, *Glob. Chang. Biol.*, 10(11), 1825–1834, doi:10.1111/j.1365-
850 2486.2004.00834.x, 2004.

851 Reeburgh, W. S.: Oceanic Methane Biogeochemistry, *Chem. Rev.*, 2, 486–513,
852 doi:10.1021/cr050362v, 2007.

853 Robertson, A. I., Alongi, D. M. and Boto, K. G.: Food chains and carbon fluxes, in
854 *Coastal and Estuarine Studies*, edited by A. I. Robertson and D. M. Alongi, pp. 293–
855 326, American Geophysical Union., 1992.

856 Rocha, A. S.: Caracterização física do estuário do rio Mojuim em São Caetano de
857 Odivelas - PA, Federal University of Pará. [online] Available from:
858 <http://repositorio.ufpa.br/jspui/handle/2011/11390>, 2015.

859 Rollnic, M., Costa, M. S., Medeiros, P. R. L. and Monteiro, S. M.: Tide Influence on
860 Suspended Matter Transport in an Amazonian Estuary, *J. Coast. Res.*, 85, 121–125,
861 doi:10.2112/SI85-025.1, 2018.

862 Rosentreter, J. A., Maher, D. T., Erler, D. V., Murray, R. H. and Eyre, B. D.: Methane
863 emissions partially offset “blue carbon” burial in mangroves, *Sci. Adv.*, 4(6), 1–11,
864 doi:10.1126/sciadv.aao4985, 2018a.

865 Rosentreter, J. A., Maher, D. . T., Erler, D. V. V., Murray, R. and Eyre, B. D. D.:
866 Seasonal and temporal CO₂ dynamics in three tropical mangrove creeks – A revision of
867 global mangrove CO₂ emissions, *Geochim. Cosmochim. Acta*, 222, 729–745,
868 doi:10.1016/j.gca.2017.11.026, 2018b.

869 Roslev, P. and King, G. M.: Regulation of methane oxidation in a freshwater wetland by
870 water table changes and anoxia, *FEMS Microbiol. Ecol.*, 19(2), 105–115,
871 doi:10.1111/j.1574-6941.1996.tb00203.x, 1996.

872 Sahu, S. K. and Kathiresan, K.: The age and species composition of mangrove forest
873 directly influence the net primary productivity and carbon sequestration potential,
874 *Biocatal. Agric. Biotechnol.*, 20, 101235, doi:10.1016/j.bcab.2019.101235, 2019.

875 Salum, R. B., Souza-Filho, P. W. M., Simard, M., Silva, C. A., Fernandes, M. E. B.,
876 Cougo, M. F., do Nascimento, W. and Rogers, K.: Improving mangrove above-ground
877 biomass estimates using LiDAR, *Estuar. Coast. Shelf Sci.*, 236, 106585,
878 doi:10.1016/j.ecss.2020.106585, 2020.

879 Schmidt, M. W. I., Torn, M. S., Abiven, S., Dittmar, T., Guggenberger, G., Janssens, I.
880 A., Kleber, M., Kögel-Knabner, I., Lehmann, J., Manning, D. A. C., Nannipieri, P.,
881 Rasse, D. P., Weiner, S. and Trumbore, S. E.: Persistence of soil organic matter as an

882 ecosystem property, *Nature*, 478(7367), 49–56, doi:10.1038/nature10386, 2011.

883 Segarra, K. E. A., Schubotz, F., Samarkin, V., Yoshinaga, M. Y., Hinrichs, K. U. and
884 Joye, S. B.: High rates of anaerobic methane oxidation in freshwater wetlands reduce
885 potential atmospheric methane emissions, *Nat. Commun.*, 6(1), 1–8,
886 doi:10.1038/ncomms8477, 2015.

887 Shiau, Y.-J. and Chiu, C.-Y.: Biogeochemical Processes of C and N in the Soil of
888 Mangrove Forest Ecosystems, *Forests*, 11(5), 492, doi:10.3390/f11050492, 2020.

889 Shiau, Y. J., Cai, Y., Lin, Y. Te, Jia, Z. and Chiu, C. Y.: Community Structure of Active
890 Aerobic Methanotrophs in Red Mangrove (*Kandelia obovata*) Soils Under Different
891 Frequency of Tides, *Microb. Ecol.*, 75(3), 761–770, doi:10.1007/s00248-017-1080-1,
892 2018.

893 Sihi, D., Davidson, E. A., Chen, M., Savage, K. E., Richardson, A. D., Keenan, T. F.
894 and Hollinger, D. Y.: Merging a mechanistic enzymatic model of soil heterotrophic
895 respiration into an ecosystem model in two AmeriFlux sites of northeastern USA,
896 *Agric. For. Meteorol.*, 252, 155–166, doi:10.1016/J.AGRFORMET.2018.01.026, 2018.

897 Souza Filho, P. W. M.: Costa de manguezais de macromaré da Amazônia: cenários
898 morfológicos, mapeamento e quantificação de áreas usando dados de sensores remotos,
899 *Rev. Bras. Geofísica*, 23(4), 427–435, doi:10.1590/S0102-261X2005000400006, 2005.

900 Sparling, G. P. and West, A. W.: A direct extraction method to estimate soil microbial
901 C: calibration in situ using microbial respiration and ¹⁴C labelled cells, *Soil Biol.*
902 *Biochem.*, 20(3), 337–343, doi:10.1016/0038-0717(88)90014-4, 1988.

903 Sundqvist, E., Vestin, P., Crill, P., Persson, T. and Lindroth, A.: Short-term effects of
904 thinning, clear-cutting and stump harvesting on methane exchange in a boreal forest,
905 *Biogeosciences*, 11(21), 6095–6105, doi:10.5194/bg-11-6095-2014, 2014.

906 Valentim, M., Monteiro, S. and Rollnic, M.: The Influence of Seasonality on Haline
907 Zones in An Amazonian Estuary, *J. Coast. Res.*, 85, 76–80, doi:10.2112/SI85-016.1,
908 2018.

909 Valentine, D. L.: Emerging Topics in Marine Methane Biogeochemistry, *Ann. Rev.*
910 *Mar. Sci.*, 3(1), 147–171, doi:10.1146/annurev-marine-120709-142734, 2011.

911 Vance, E. D., Brookes, P. C. and Jenkinson, D. S.: An extraction method for measuring
912 soil microbial biomass C, *Soil Biol. Biochem.*, 19(6), 703–707, doi:10.1016/0038-

913 0717(87)90052-6, 1987.

914 Verchot, L. V., Davidson, E. A., Cattânio, J. H. and Ackerman, I. L.: Land-use change
915 and biogeochemical controls of methane fluxes in soils of eastern Amazonia,
916 *Ecosystems*, 3(1), 41–56, doi:10.1007/s100210000009, 2000.

917 Wang, X., Zhong, S., Bian, X. and Yu, L.: Impact of 2015–2016 El Niño and 2017–
918 2018 La Niña on PM_{2.5} concentrations across China, *Atmos. Environ.*, 208, 61–73,
919 doi:10.1016/J.ATMOSENV.2019.03.035, 2019.

920 Whalen, S. C.: Biogeochemistry of Methane Exchange between Natural Wetlands and
921 the Atmosphere, *Environ. Eng. Sci.*, 22(1), 73–94, doi:10.1089/ees.2005.22.73, 2005.

922 Xu, X., Elias, D. A., Graham, D. E., Phelps, T. J., Carroll, S. L., Wulfschleger, S. D. and
923 Thornton, P. E.: A microbial functional group-based module for simulating methane
924 production and consumption: Application to an incubated permafrost soil, *J. Geophys.
925 Res. Biogeosciences*, 120(7), 1315–1333, doi:10.1002/2015JG002935, 2015.

926